



Understanding meteorological and physio-geographical controls of variability of flood event classes in China

Yongyong Zhang¹, Yongqiang Zhang¹, Xiaoyan Zhai², Jun Xia^{3,1}, Qihong Tang¹, Wei Wang¹, Jian Wu¹, Xiaoyu Niu¹, Bing Han¹

5 ¹Key Laboratory of Water Cycle and Related Land Surface Processes, Institute of Geographic Sciences and Natural Resources Research, Chinese Academy of Sciences, Beijing, 100101, China.

²China Institute of Water Resources and Hydropower Research, Beijing, 100038, China.

³State Key Laboratory of Water Resources and Hydropower Engineering Science, Wuhan University, Wuhan, 430072, China.

10 *Correspondence to:* Yongyong Zhang (zhangyy003@igsnr.ac.cn)

Abstract. Classification is beneficial for understanding flood variabilities and their formation mechanisms from massive flood event samples for both flood scientific research and management purposes. Our study investigates spatial and temporal variabilities of 1446 unregulated flood events in 68 headstream catchments in China at class scale using hierarchical and partitional clustering methods. Control mechanisms of meteorological and physio-geographical factors (e.g., meteorology, 15 land cover and catchment attributes) are explored for individual flood event classes using constrained rank analysis and Monte Carlo permutation test. Results show that we identify five robust flood event classes, i.e., moderately, highly, and slightly fast floods, as well as moderately and highly slow floods, which accounts for 24.0%, 21.2%, 25.9%, 13.5% and 15.4% of total events, respectively. All the classes are evenly distributed in the whole period, but the spatial distributions are quite distinct. The fast flood classes are mainly in the southern China, and the slow flood classes are mainly in the northern China and the 20 transition region between southern and northern China. The meteorological category plays a dominant role in flood event variabilities, followed by catchment attributes and land covers. Precipitation factors, such as volume and intensity, and aridity index are the significant control factors. Our study provides insights into flood event variabilities and aids in flood prediction and control.

1 Introduction

25 Flood events usually show tremendous spatial and temporal variabilities in behavior due to heterogeneities in meteorological and underlying surface conditions over large basins or entire regions (e.g., county, continent and world) (Berger and Entekhabi, 2001). It is a huge effort and unrepresentative to investigate the flood change characteristics at event scale (Tarasova *et al.*, 2019; Zhang *et al.*, 2020). Flood event similarity analysis is beneficial to investigate comprehensive dynamic characteristics of flood events in space and time by grouping massive homogeneous events into some manageable classes with significantly 30 statistical differences of flood behaviors (e.g., great or small floods, fast or slow floods, rain or snowmelt floods) (Brunner, 2018). Flood event class determines hydrological response characteristics, longitudinal and lateral transfers of energy and



material, and structures and functions of riverine ecosystems (Arthington *et al.*, 2006; Poff and Zimmerman, 2010). The class also directly determines flood disaster losses for human society and affects the strategy formulations of flood control and management (Hirabayashi *et al.*, 2013; Jongman *et al.*, 2015). Hence, for both flood scientific research and management
35 purposes, it is fundamentally important to identify the flood event classes and their formation mechanisms (Sikorska *et al.*, 2015).

Inductive and deductive approaches are reported for the flood event similarity classification according to the clustering objectives (Olden *et al.*, 2012). The inductive approach directly focuses on the shape similarity of flood events by clustering
40 the behavior characteristics extracted from the flood event hydrographs. The behavior characteristics include magnitude, frequency, duration, timing and seasonality, variability metrics, which are considered as the critical components to characterize the entire range of flood events (Poff *et al.*, 1997; Kuentz *et al.*, 2017; Zhang *et al.*, 2020). The reported flood event classes are the fast events with steep rising and falling limbs, the slow events with both elongated rising and falling limbs, the sharp or fast flood event, the flash flood (Kuentz *et al.*, 2017; Brunner *et al.*, 2018; Zhai *et al.*, 2021; Zhang *et al.*, 2020). The deductive
45 approach mainly focuses on the similarity of environmental factors assumed to control flood events, such as meteorological variables (e.g., storm intensity, duration and snowmelt) and physio-geographical conditions (e.g., soil moisture, land cover and topography) (Merz and Blöschl, 2003; Ali *et al.*, 2012; Brunner *et al.*, 2018; Zhang *et al.*, 2022). The reported flood event classes are the long-rain floods, short-rain floods, flash floods, rain-on-snow floods, and snowmelt floods (Merz and Blöschl, 2003; Sikorska *et al.*, 2015; Brunner *et al.*, 2018; Zhang *et al.*, 2022). However, the control relationships of environmental
50 factors on flood event shapes are not well defined so that the identified classes are not exactly helpful to investigate the flood change patterns at event scale. Therefore, it is a challenge to better understand the formation mechanisms of individual flood event classes.

The main procedure of existing flood event classification was to cluster the similarity of flood event attributes (e.g., flood
55 behavior characteristics or control factors) across the spatial and temporal scales. According to the classification procedure, there are two widely-adopted approaches: the hierarchical clustering methods (e.g., single linkage, complete linkage, average linkage, centroid linkage, ward linkage) and partitional clustering methods (e.g., *k*-mean, *k*-medoids, decision tree) (Kennard *et al.*, 2010; Olden *et al.*, 2012; Sikorska *et al.*, 2015; Zhang *et al.*, 2020; Zhai *et al.*, 2021). The hierarchical clustering methods are simple but determining the clustering number is usually subjective according to the dendrogram, and are difficult to solve
60 the classification of a large number of flood events (Olden *et al.*, 2012; Zhang *et al.*, 2020). The partitional clustering methods are efficient to large sample classification, but require to predefine the clustering number or the thresholds of flood event attributes by users (Hartigan and Wong, 1979; Sikorska *et al.*, 2015; Zhai *et al.*, 2021). Additionally, the determinations of clustering method and final cluster number are subjective in most existing studies, and the assessment of clustering performance is usually unavailable (Olden *et al.*, 2012; Sikorska *et al.*, 2015; Brunner *et al.*, 2017). Therefore, robustness of
65 flood event classification should be further explored.



The main aim of this study is to investigate the flood event similarity and the control mechanisms of meteorological and physio-geographical factors in space and time at class scale in China. Over one thousand unregulated flood events at 68 sites from six major basins in China are selected for our study. The specific objectives are as follows:

- 70 (i) to determine the optimal flood event classes by comparing multiple classification performance criteria of both the hierarchical and partitional clustering methods;
- (ii) to identify the main flood behavior characteristics of individual classes and their spatial and temporal variabilities;
- (iii) to quantify the effects of meteorological and physio-geographical factors on the variabilities of individual flood event classes.

75

This study provides insights into the comprehensive change patterns and their formation mechanisms of flood events, and provides a solid data foundation for predicting flood event classes.

2 Study area and data sources

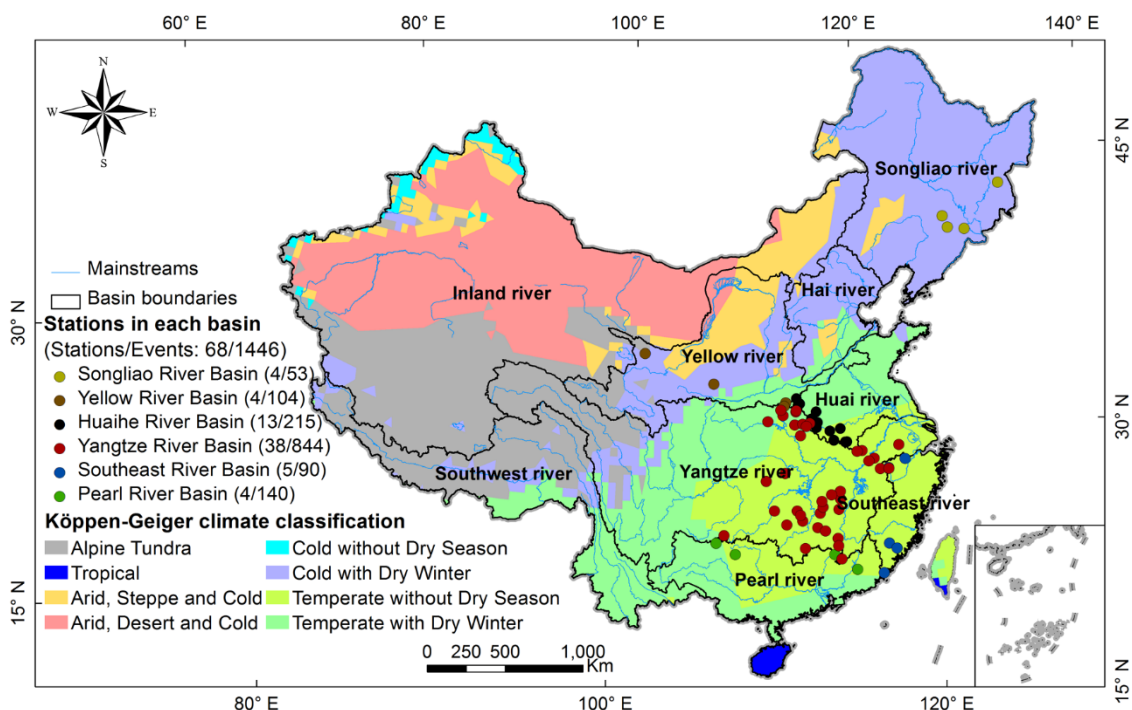
According to the Köppen-Geiger climate classification (Peel *et al.*, 2007), China has diverse climate types, including alpine
80 tundra climate (ET for Köppen-Geiger codes), tropical climate (A), arid, steppe and cold climate (BSk), arid, desert and cold (BWk), cold without dry season (Df), cold with dry winter (Dw), temperate without dry season (Cf) and temperate with dry winter (Cw). Most Köppen-Geiger climate types in China (i.e., A, Df, Dw, Cf and Cw) are controlled by the southeast and southwest monsoons in the summer with temperate and humid climates and the northwestern and northeastern monsoons in the winter with cold and dry climates. In these climate types, the mean annual precipitation was 365-2654 mm with a mean of
85 1184 mm, of which over 65% fell between May and September according to the gauged daily precipitation observations from 2001 to 2020 in these regions. This led to frequent flooding. In the last decade, flooding occurred in 455 rivers annually, which affected 822 million people and averaged over 10 billion US dollars (Ministry of Water Resources of the People's Republic of China, 2020a).

90 Sixty-eight headstream stations were selected with catchment areas ranging from 21 km² to 4830 km², which were mainly located in flood-prone areas of China (Figure 1). Most catchments had large forest coverage, with mean area percentages of 67.0%, particularly in the Yangtze (69.9%) and Pearl (68.7%) River Basins. A total of 1446 unregulated flood events with hourly time steps were collected from the Hydrological Yearbooks of the Songliao, Yellow, Huaihe, Yangtze, Southeast and Pearl River Basins over the period 1993—2015 (http://xxfb.mwr.cn/sq_djdh.html). The event was extracted following the
95 Standard of Ministry of Water Resources of the People's Republic of China, i.e., Code for hydrologic data processing (SL/T 247—2020) (Ministry of Water Resources of the People's Republic of China, 2020b). The extracted flood events at the individual stations usually had the maximum flood peak or flood volume, isolated flood peak, continuous flood peaks, or flood



100 peak after prolonged drought during the high and normal flow years (Ministry of Water Resources of the People's Republic
of China, 2020b). There were 53 events at four stations in the Songliao River Basin, 104 events at four stations in the Yellow
River Basin, 215 events at 13 stations in the Huaihe River Basin, 844 events at 38 stations in the Yangtze River Basin, 90
events at five stations in the Southeast River Basin, and 140 events at four stations in the Pearl River Basin. No less than 10
flood events were collected for every station to ensure the representativeness.

Meteorological, catchment and land cover data sources were collected together to assess the potential meteorological and
105 physio-geographical control factors of flood events. The meteorological data sources were the synchronous hourly
precipitation events which were also extracted from the Hydrological Yearbooks (http://xxfb.mwr.cn/sq_djdh.html), and the
daily precipitation, maximum and minimum temperature observations from 1993 to 2015 at 466 meteorological stations within
or around the catchments which were downloaded from the China Meteorological Data Sharing Service System
(<http://cdc.cma.gov.cn/home.do>). The daily meteorological variables were interpolated to the catchment by the inverse distance
110 weighting method. The geographic information system data were collected to extract the attributes of catchment and land cover.
The detailed data were the digital elevation model with a spatial resolution of 30 m×30 m and land covers in six periods (i.e.,
1990, 1995, 2000, 2005, 2010 and 2015) with a spatial resolution of 30 m×30 m, all of which were downloaded from the Data
Sharing Infrastructure of Earth System Science (<http://www2.geodata.cn/index.html>).



115 **Figure 1. Spatial distributions of all the selected flood events and their corresponding climate types**



3 Methods

3.1 Flood behavior metrics

The flood classification in our study mainly focuses on the detailed behavior characteristics of flood hydrographs by the inductive approach. The magnitude, variability, timing, duration, and rate of changes are adopted to characterize the detailed flood behaviors (Poff *et al.*, 2007). Additionally, flood peak number is one of the most important metrics for flood control (Aristeidis *et al.*, 2010; Rustomji *et al.*, 2009). Therefore, nine metrics are used to capture the behavior of flood events. There are the magnitude (total flood volume: R , maximum flood peak: Q_{pk}), variability (coefficient of variation: CV), timing (timings of flood event and maximum flood peak: T_{bgn} and T_{pk}), duration (flood event duration: T_{drm}), rate of changes (mean rates of positive and negative changes: RQ_r and RQ_d) and flood peak number (N_{pk}) (Arthington *et al.*, 2006; Kennard *et al.*, 2010; Poff *et al.*, 2007; Zhang *et al.*, 2012). Table 1 summarizes the definitions of all the selected flood components.

Table 1. Metrics used to characterize flood behaviors in our study

Components	Metrics	Abbreviations	Units	Equations	References
Magnitude	Total flood volume	R	$\text{mm}\cdot\text{day}^{-1}$	$R = 86.4 \cdot \sum_{t=TF_{bgn}}^{TF_{end}} Q_t / A$	
	Maximum flood peak	Q_{pk}	$\text{mm}\cdot\text{day}^{-1}$	$Q_{pk} = \max(86.4 \cdot Q_t) / A$	
Variability	Coefficient of variation	CV	-	$CV = \sigma / Q_{av}$	
Timing	Ratio of beginning date of flood event in the calender year using circular statistics	T_{bgn}	radian	$T_{bgn} = 2\pi \cdot TF_{bgn} / TD$	Poff <i>et al.</i> , 2007; Hall and Blöschl, 2018; Zhang <i>et al.</i> , 2020
	Ratio of occurrence day of maximum flood peak to flood duration	T_{pk}	%	$T_{pk} = TF_{pk} / T_{drm} \cdot 100$	
Duration	Duration of flood event	T_{drm}	h	$T_{drm} = 24 \cdot (TF_{end} - TF_{bgn} + 1)$	
Rate of changes	Mean rate of positive changes	RQ_r	h^{-1}	$RQ_r = \frac{(Q_{pk} - Q_{bgn}) / Q_{av}}{(TF_{pk} - TF_{bgn} + 1) \cdot 24}$	
	Mean rate of negative changes	RQ_d	h^{-1}	$RQ_d = \frac{(Q_{pk} - Q_{end}) / Q_{av}}{(TF_{end} - TF_{pk} + 1) \cdot 24}$	
Number	Number of peaks during the event	N_{pk}	-		Aristeidis <i>et al.</i> , 2010; Zhai <i>et al.</i> , 2021

Note: Q_t is the flood magnitude on day t ($\text{m}^3\cdot\text{s}^{-1}$); Q_{av} is the mean flood magnitude ($\text{m}^3\cdot\text{s}^{-1}$); Q_{bgn} and Q_{end} are flood magnitudes at the beginning and end of event ($\text{m}^3\cdot\text{s}^{-1}$), respectively; σ is the standard deviation of flood magnitude ($\text{m}^3\cdot\text{s}^{-1}$); TD is the total days of the calendar year (day), i.e., 365 for common year or 366 for leap year; TF_{bgn} and TF_{end} are the beginning and end dates



of flood events; TF_{pk} is the occurrence date of maximum flood peak; A is the catchment area (km^2); 86.4 is the unit conversion factor from $\text{m}^3 \cdot \text{s}^{-1} \cdot \text{km}^{-2}$ to mm.

3.2 Flood event classification

135 High dimensionality and multicollinearity exist among flood behavior metrics and affect the flood event classification when a
large number of metrics are considered (Olden *et al.*, 2012; Zhang *et al.*, 2012). Dimensionality reduction is to transform the
high dimensional metrics into a few independent composite metrics without losing the metric information, and to reveal the
major similarity characteristics among the metrics. Here, principal component analysis is used to obtain a few principal
components (*PCA*) based on the orthogonal transform. If the cumulative variance is over 85% of the total variances of all the
140 *PCAs*, the first m *PCAs* are selected for classification.

Subsequently, both the hierarchical (Ward's) and partitional (k -medoids) clustering methods are used to cluster flood events
based on the similarity of the selected *PCAs*. Euclidean distance is the distance measure used. Twenty-two criteria are used to
assess the classification performance and determine the best number of clusters, i.e., KL, CH, Hartigan, CCC, Scott, Marriot,
145 TrCovW, TraceW, Friedman, Silhouette, Ratkowsky, Ball, Ptbiserial, Dunn, Rubin, Cindex, DB, Duda, Pseudot2, McClain,
SDindex and SDbw (Charrad *et al.*, 2014). The greater values of the first fourteen indexes (i.e., KL to Dunn) or the smaller
values of the rest eight criteria (i.e., Rubin to SDbw) indicate the better classification. If the best criteria number is the largest
in a certain cluster number, the cluster number is optimal and the corresponding clustering method is also selected.

150 All the multivariable statistical analyses are implemented using R software (version 3.1.1) (R Development Core Team, 2010),
involving the `princomp` function in stats Package (version 4.1.3) for principal component analysis (Mardia *et al.*, 1979), the
`hcluster` function in amap Package (version 0.8-18) for hierarchical cluster analysis (Antoine and Sylvain, 2006), the
`clara` function in cluster Package (version 2.1.3) for k -medoids cluster analysis (Kaufman and Rousseeuw, 1990), the
`NbClust` function in NbClust Package (version 3.0.1) for the optimal class number determination and classification
155 performance assessment (Charrad *et al.*, 2014).

3.3 Control mechanisms of meteorological and physio-geographical factors on the variabilities of flood event classes

3.3.1 Meteorological and physio-geographical factors

The meteorological (e.g., storm intensity, timing and duration, evapotranspiration volume) and physio-geographical factors
160 (e.g., land covers and catchment attributes) directly affect the flood generation and routing processes, which thus cause the
diversity of flood event shapes (Ali *et al.*, 2012; Brunner *et al.*, 2018; Merz and Blöschl, 2003; Zhang *et al.*, 2022). A total of



34 meteorological, catchment and land cover factors in all the catchments are selected to investigate the control mechanisms on the variability of flood event classes. In the meteorological category, 17 factors related to precipitation, potential evapotranspiration and aridity index are selected, including the factors during flood events (i.e., total and mean amounts, maximum intensity, timing and duration of precipitation: pcp_dur, pcp_av, pcp_max, pcp_Tbeg and pcp_Tdur; total and maximum potential evapotranspiration: pet_dur and pet_max; aridity index: SPEI_dur), in the antecedent seven days (i.e., pcp_ant, pet_ant and SPEI_ant), and at annual scale (i.e., annual mean factors: pcp_ann, pet_ann and SPEI_ann; factors in the year when the flood event happens: pcp_year, pet_year and SPEI_year). All the precipitation factors during the flood events are extracted using the hourly precipitation observations. The precipitation factors at daily or annual scale are extracted using the daily precipitation observations. The potential evapotranspiration at daily or annual scale is estimated using the Hargreaves method (Hargreaves and Samani, 1982), and the aridity index is the ratio of potential evapotranspiration to precipitation.

For the physio-geographical factors, the 10 catchment attributes are selected, including longitude, latitude and elevation of catchment center, catchment area, mean slope and length, maximum elevation, river density and slope, ratio of river width to depth (i.e., Longitude, Latitude, Elevation, Area, Slope, Length, MaxiElev, Rivden, RivSlope and Rwd). Seven land cover factors are selected, including the area fractions of paddy, dryland, forest, grassland, water, urban and rural area to the total catchment (i.e., Rpaddy, Rdryland, Rforest, Rgrass, Rwater, Rurban and Rrural), respectively for the seven land cover periods. All these factors are extracted using the Hydrology and Zonal functions of the Spatial Analyst Tools in the ArcGIS Desktop (version 10.0).

Table 2. Metrics used to characterize flood behaviors in our study

Factor categories	Factors	Data sources	Flood effects	event	
Meteorology	Precipitation	Cumulative amount in the antecedent seven days (pcp_ant, mm); total and mean amounts (pcp_dur, mm; pcp_av, mm hr ⁻¹), maximum intensity (pcp_max, mm hr ⁻¹), timing (pcp_Tbeg) and duration (pcp_Tdur, days) during the flood event, annual mean amount (pcp_ann, mm) and amount in the year when the flood event happens (pcp_year, mm)	Hourly precipitation in hydrological yearbooks; daily precipitation from 1993 to 2015 at 466 meteorological stations	Flood process	yield
	Potential evapotranspiration	Cumulative amount in the antecedent seven days (pet_ant, mm); total amount (pet_dur, mm), maximum intensity (pet_max, mm hr ⁻¹) during the flood event, annual mean amount (pet_ann, mm) and amount in the year when the flood event happens (pet_year, mm)	Daily maximum and minimum temperature from 1993 to 2015 at 466 meteorological stations	Flood process	yield



	Aridity index	Mean values in the antecedent seven days (SPEI_ant), during the flood event (SPEI_dur), in the many years (SPEI_ann) and in the year when the flood event happens (SPEI_year)	Daily maximum and minimum temperature from 1993 to 2015 at 466 meteorological stations	Flood yield process
	Locations	Longitude and latitude (Longitude and Latitude)	Global positioning system	Meteorological conditions
Physio-geography	Catchment attributes	Slope (Slope, %), area (Area, km ²), length (Length, km), average and maximum elevation (Elevation, m; MaxiElev, m)	Digital elevation model (size: 30 m×30 m)	Flood yield and overland routing processes
	River attributes	River density (Rivden, km/km ²), Slope (RivSlope, %) and width-depth ratio (Rwd, m/m),	Digital elevation model (size: 30 m×30 m)	Flood routing processes in river system
	Land covers	Area fractions of Paddy (Rpaddy, %), dryland (Rdryland, %), forest (Rforest, %), grass (Rgrass, %), water (Rwater, %), urban (Rurban, %) and unused land (Rrural, %) to the total catchment	Land covers in 1990, 1995, 2000, 2005, 2010 and 2015 (size: 30 m×30 m)	Flood yield and overland routing processes

3.3.2 Effect quantifications of meteorological and physio-geographical factors

The constrained rank analysis is adopted to quantify the direct or combined effects of control factor categories on spatial and temporal variabilities of individual flood event classes for the distributed and lumped analyses, respectively. It is beneficial to quantify the effects of explanatory metrics on a response metrics and to find the most important factors, which has been commonly used in testing the multispecies response to environmental variables in the biological or ecological sciences (Legendre and Anderson, 1999), effects of physio-geographical factors and human activities on diffuse nutrient losses or water quality (Zhang *et al.*, 2016; Shi *et al.*, 2017), and so on. The widely adopted methods of constrained rank analysis are the Redundancy Analysis (RDA) and the Canonical Correlation Analysis (CCA) which are selected based on the first axis length. The CCA is proposed when the first axis length is greater than 4.0, while the RDA is proposed when the first axis length is less than 3.0. Otherwise, both CCA and RDA are proposed (ter Braak, 1986; Zhang *et al.*, 2020). The constrained proportion is the effect contribution of individual meteorological and physio-geographical factors or categories on total variabilities of flood event classes. If the contribution sum of individual factor effects is less than the entire contribution of all the factors, the interactive effects are among the factors and the difference between the summed and entire contributions is the combined contribution (Zhang *et al.*, 2016).

Furthermore, the Monte Carlo permutation test is adopted to test the statistical significance of control factors on the variability of flood event classes, and obtain the correlation coefficients (*r*) between flood behavior matrix and control factor matrix in the individual catchments (i.e., distributed analysis) and the entire region (i.e., lumped analysis), respectively. Because all the



catchment factors do not change in the entire period, only the meteorological and land cover categories are considered for the correlation relationship test for the lumped analysis. The significant statistical interval is set as 95%, i.e., $p=0.05$. The above-mentioned analyses are implemented using the `envfit`, `decorana`, `rda`, `cca`, `permutest` functions in the `vegan` Package (version 2.5-7) of R software (version 3.1.1) (ter Braak, 1986; R Development Core Team, 2010).

205 4 Results

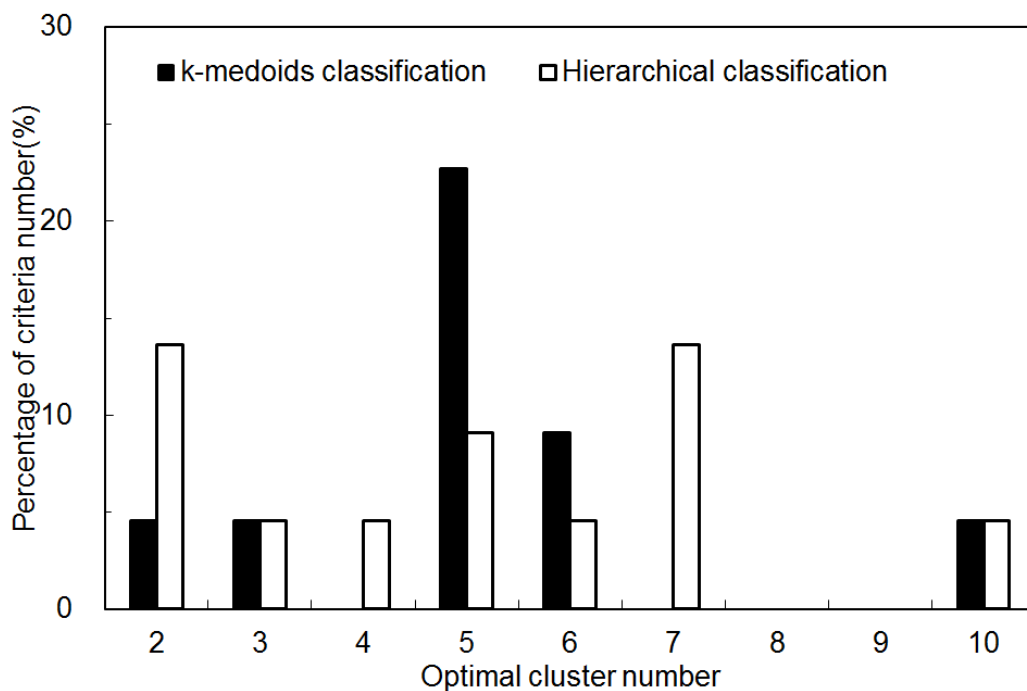
4.1 Flood event classification

For all the flood behavior metrics, five independent *PCAs* are found with the total cumulative variance of 85.7% (Table 3). The first *PCA* is related with magnitude (R and Q_{pk}), variability (CV) and rates of changes (RQ_r and RQ_d) with the variances of 33.2%, and the second - fifth *PCAs* are mainly related with flood peak number (N_{pk}), duration (T_{drm}), timings (T_{bgn} and T_{pk}) of flood event and maximum flood peak with the variances of 17.0%, 16.0%, 10.8% and 8.6%, respectively.

Compared with the classification performance of these two clustering methods among individual optimal cluster numbers (Figure 2), the optimal criteria number is the largest when the optimal cluster number is five (i.e., 22.7% of total) for the k -medoids clustering method. The optimal criteria are the CCC, TrCovW, Silhouette, Ratkowsky and PtBiserial with the values of -2.98, 1.39×10^{15} , 4.12×10^6 , 0.20, 0.29 and 0.39, respectively. Therefore, the five clusters using the k -medoids clustering method are optimum for further analysis in our study. The flood event numbers in the individual classes are 347, 306, 195, 375 and 223, accounting for 24.0%, 21.2%, 13.5%, 25.9% and 15.4% of total events, respectively.

Table 3. Flood behavior metrics in the selected PCAs and their variances

Metrics	PCA1	PCA2	PCA3	PCA4	PCA5
R	0.61	0.51	0.30	-0.01	0.06
Q_{pk}	0.97	0.08	0.00	-0.02	0.02
CV	0.47	-0.47	0.42	-0.28	0.40
T_{bgn}	0.05	-0.22	0.26	0.92	0.16
T_{pk}	-0.07	0.56	-0.48	0.03	0.64
T_{drm}	-0.19	0.16	0.84	-0.13	0.20
RQ_r	0.84	-0.22	-0.06	-0.01	-0.18
RQ_d	0.84	0.05	-0.29	0.10	0.02
N_{pk}	0.07	0.77	0.30	0.10	-0.31
Variance (%)	33.3	17.0	16.0	10.8	8.6
Cumulative variance (%)	85.7				



220

Figure 2. Classification performance comparisons between the hierarchical and *k*-medoids methods among individual optimal cluster numbers

4.2 Flood behavior characteristics of different classes

225

For the magnitude metrics (Figure 3), both total flood volume (R) and maximum flood peak (Q_{pk}) variations are the same among different classes, and the values from large to small are 144.0 ± 108.3 mm and 5.2 ± 6.0 mm in Class 3, followed by 65.8 ± 43.8 mm and 3.0 ± 3.7 mm in Class 5, 45.8 ± 34.0 mm and 2.2 ± 2.5 mm in Class 2, 44.0 ± 29.9 mm and 2.0 ± 2.5 mm in Class 1, 33.3 ± 26.6 mm and 1.7 ± 2.1 mm in Class 4, respectively. For the variability metrics (CV), the events are the most variable in Class 5 with the mean of 1.40 ± 0.43 , and are more variable in the other Classes with the mean of 0.90 ± 0.26 (Class 1), 0.87 ± 0.25

230

(Class 2), 0.86 ± 0.26 (Class 4) and 0.84 ± 0.22 (Class 3), respectively.

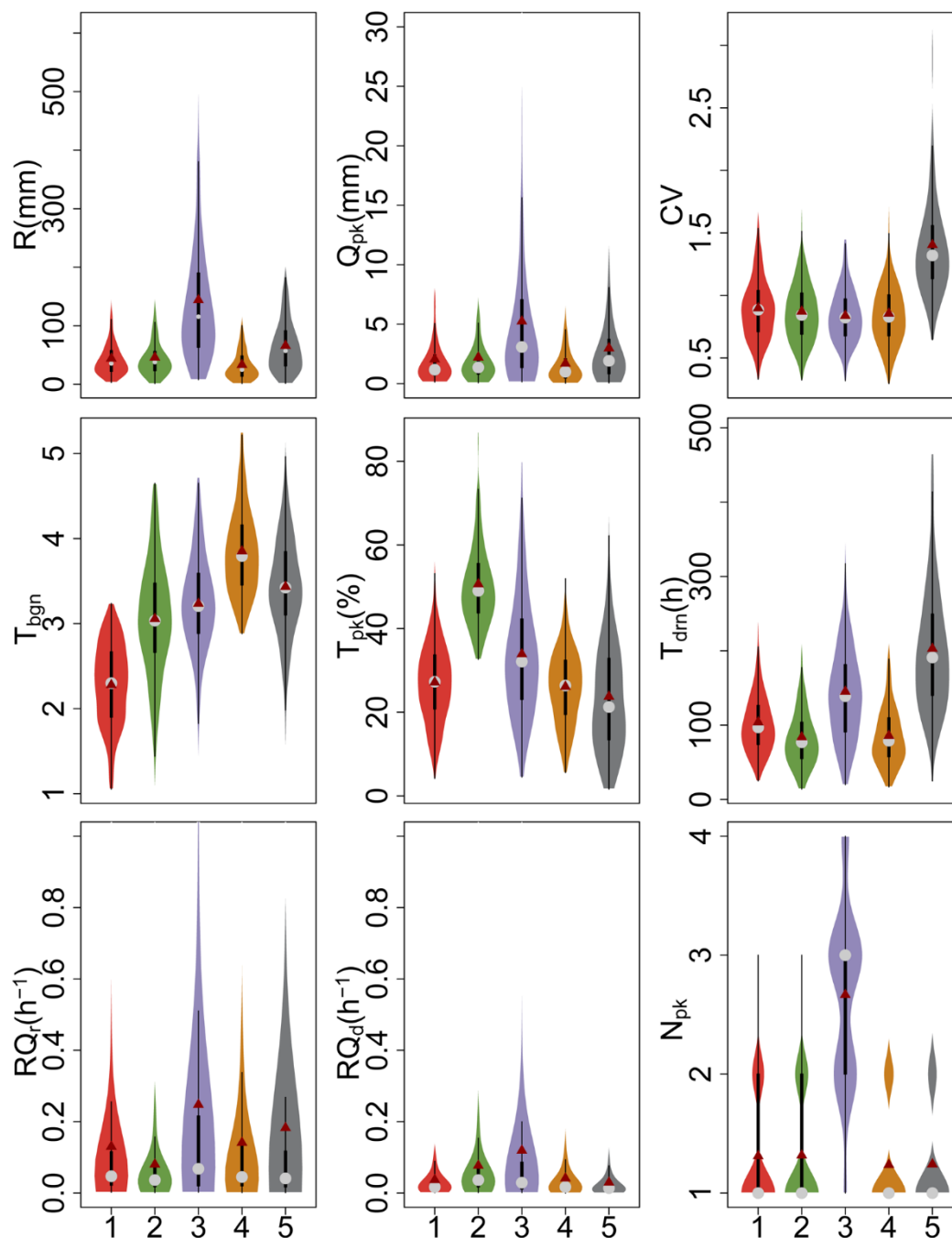


Figure 3. Variations of flood behavior metrics among Classes 1-5. The solid dark red dot and gray dot define the mean and 50th percentile values, respectively. Each black box means the 25th and 75th percentile values, and the vertical line defines the minimum and maximum values without outliers. The violin shape means the frequency distribution of flood behavior metric.



For the timing and duration metrics, 73.2% of flood events in Class 1 occur before the wet season (i.e., January - May) with the mean flood event timings (T_{bgn}) of 2.28 ± 0.49 ; 58.5%, 67.7% and 57.0% of flood events in Classes 2, 3 and 5 occur in the earlier wet season (i.e., June - July) with the mean flood event timings (T_{bgn}) of 3.06 ± 0.69 , 3.24 ± 0.61 and 3.43 ± 0.61 , respectively; and 52.8% of flood events in Class 4 occur in the latter wet season (i.e., August - September) with the the mean
240 flood event timings (T_{bgn}) of 3.85 ± 0.51 . The flood event durations (T_{drn}) are the largest in Class 5 with the mean of 8.45 ± 3.56 days, followed by Classes 3 (6.05 ± 2.87 days), 1 (4.33 ± 1.81 days), 4 (3.57 ± 1.67 days) and 2 (3.49 ± 1.72 days). The timings of maximum flood peaks (T_{pk}) are the largest in Class 2 with the mean of $50.6\% \pm 10.3\%$, which means that the flood peaks mainly occur in the middle or late stages of flood events. The flood peaks usually occur in the early stage of flood events in the other classes with the mean timings of maximum flood peaks (T_{pk}) of $23.7\% \pm 13.6\%$ (Class 5), $26.1\% \pm 9.1\%$ (Class 4), $27.1\% \pm 9.6\%$
245 (Class 1), and $33.9\% \pm 15.0\%$ (Class 3).

For the rates of changes, the mean rates of positive changes (RQ_r) in most classes are greater than the mean rates of positive changes (RQ_d) because the flood peaks usually occur in the early stage of flood events, except Class 2. The largest values of both RQ_r and RQ_d are in Class 3 with the mean of $0.25 \pm 0.62 \text{ h}^{-1}$ and $0.12 \pm 0.28 \text{ h}^{-1}$ respectively, followed by Classes 5
250 ($0.18 \pm 0.62 \text{ h}^{-1}$), 4 ($0.14 \pm 0.30 \text{ h}^{-1}$), 1 ($0.13 \pm 0.32 \text{ h}^{-1}$) and 2 ($0.08 \pm 0.14 \text{ h}^{-1}$) for RQ_r , and followed by Classes 2 ($0.08 \pm 0.12 \text{ h}^{-1}$), 4 ($0.04 \pm 0.08 \text{ h}^{-1}$), 1 ($0.04 \pm 0.07 \text{ h}^{-1}$) and 5 ($0.03 \pm 0.04 \text{ h}^{-1}$) for RQ_d , respectively. For the N_{pk} , 71.2%, 69.9%, 76.5% and 77.1% of flood events has one flood peaks in Classes 1, 2, 4 and 5, respectively, and multiple flood peaks (i.e., two - four) exist in 94.4% of total flood events in Class 3, accounting for 33.8% (two peaks), 48.7% (three peaks) and 11.8% (four peaks), respectively.

255 Class 1 is for moderately fast flood events occurring before the wet season, characterized by a single peak and moderate duration, referred to as the "moderately fast flood event class" (Figure 4). Class 2 represents highly fast flood events with a single peak in the late stage and short duration, denoted as the "highly fast flood event class". Class 3 exhibits highly slow flood events during the latter part of the wet season, featuring multiple peaks and long duration, known as the "highly slow and multipeak flood event class". Class 4 reflects slightly fast flood events occurring in the latter wet season with a single peak and short duration, named the "slightly fast flood event class". Lastly, Class 5 displays moderately slow flood events with a
260 single peak and long durations, designated as the "moderately slow flood event class".

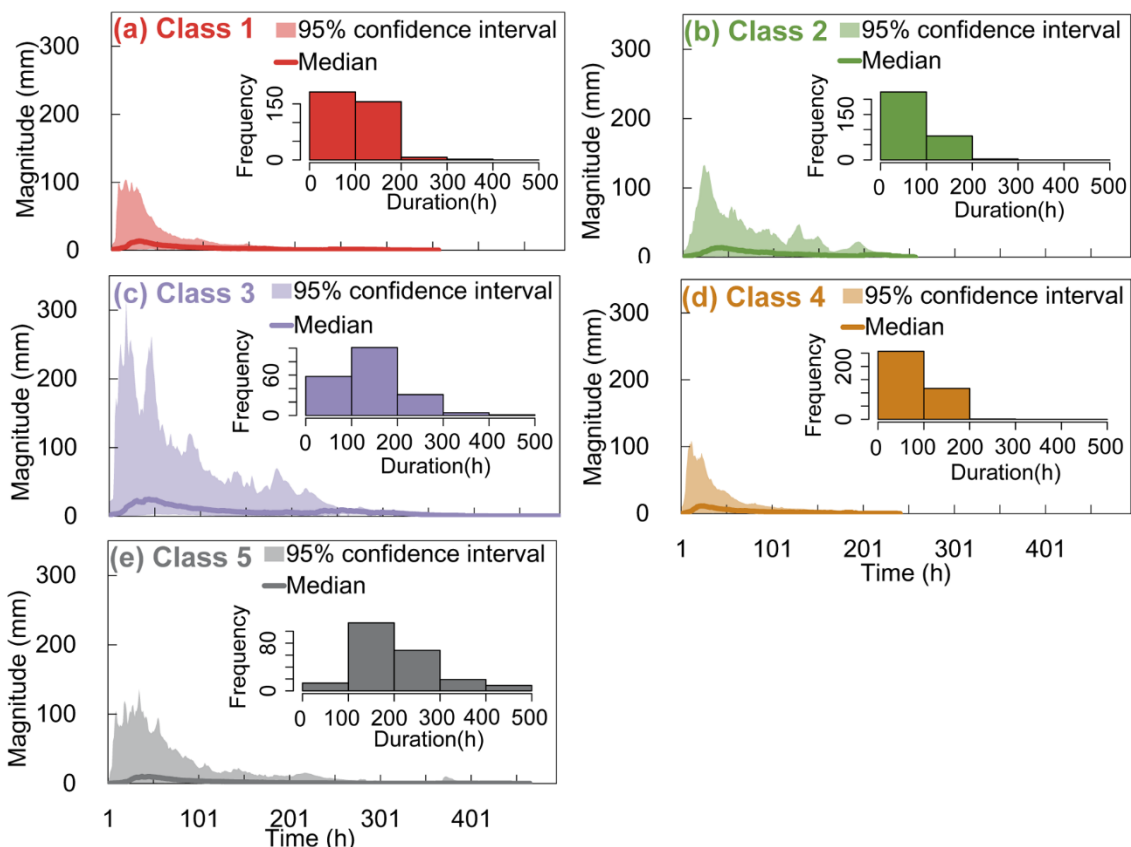


Figure 4. Flood event distributions in the 95% confidence interval and their median, and their duration frequencies of Classes 1-5

265 (a-e)

4.3 Spatial and temporal distributions of flood event classes

The spatial distributions of individual classes in the major river basins are showed in Figure 5. The moderately fast flood event class (i.e., Class 1) is mainly in the Pearl and Yangtze River Basins, accounting for 37.1% (52/140) and 29.7% (251/844) of total events, respectively. Specifically, Class 1 is dominant at the Xiawan (XW, 54.5%, 6/11) and Yanling (YL, 54.5%, 18/33) in the Yangtze River Basin. The highly fast flood event class (i.e., Class 2) is mainly in the Pearl River Basin, accounting for 31.4% (44/140) of total events, particularly in the Xiaogulu (XL, 80.0%, 24/30) catchment. The highly slow and multipeak flood event class (i.e., Class 3) is mainly in the Southeast River Basin, accounting for 42.2% (38/90) of total events, particularly in the Longshan (LS, 69.6%, 16/23) catchment. The slightly fast flood event class (i.e., Class 4) is mainly in the Yellow and Songliao River Basins, accounting for 64.4% (67/104) and 60.4% (32/53) of total events, respectively. The most obvious catchments are Biyang (BY, 83.3%, 10/12) in the Yangtze River Basin, Qiaotou (QT, 77.3%, 17/22) and Luanchuan (LC, 69.2%, 27/39) in the Yellow River Basin, Jingyu (JY, 69.2%, 9/13) and Dongfeng (DF, 64.3%, 9/14) in the Songliao River



Basin. The moderately slow flood event class (i.e., Class 5) is mainly in the Huaihe River Basin, accounting for 47.4% (102/215) of total events, particularly in the Beimiaoji (BM, 100%, 12/12) and Qilin (QL, 70.0%, 7/10) catchments. Therefore, the Classes 1 to 3 are mainly in the Temperate without Dry Season climate region in southern China (Figure 1), the Class 4 is mainly in the Cold with Dry Winter climate region in northern China, and the Class 5 is mainly in the transition region between Temperate without Dry Season climate and Cold with Dry Winter climate.

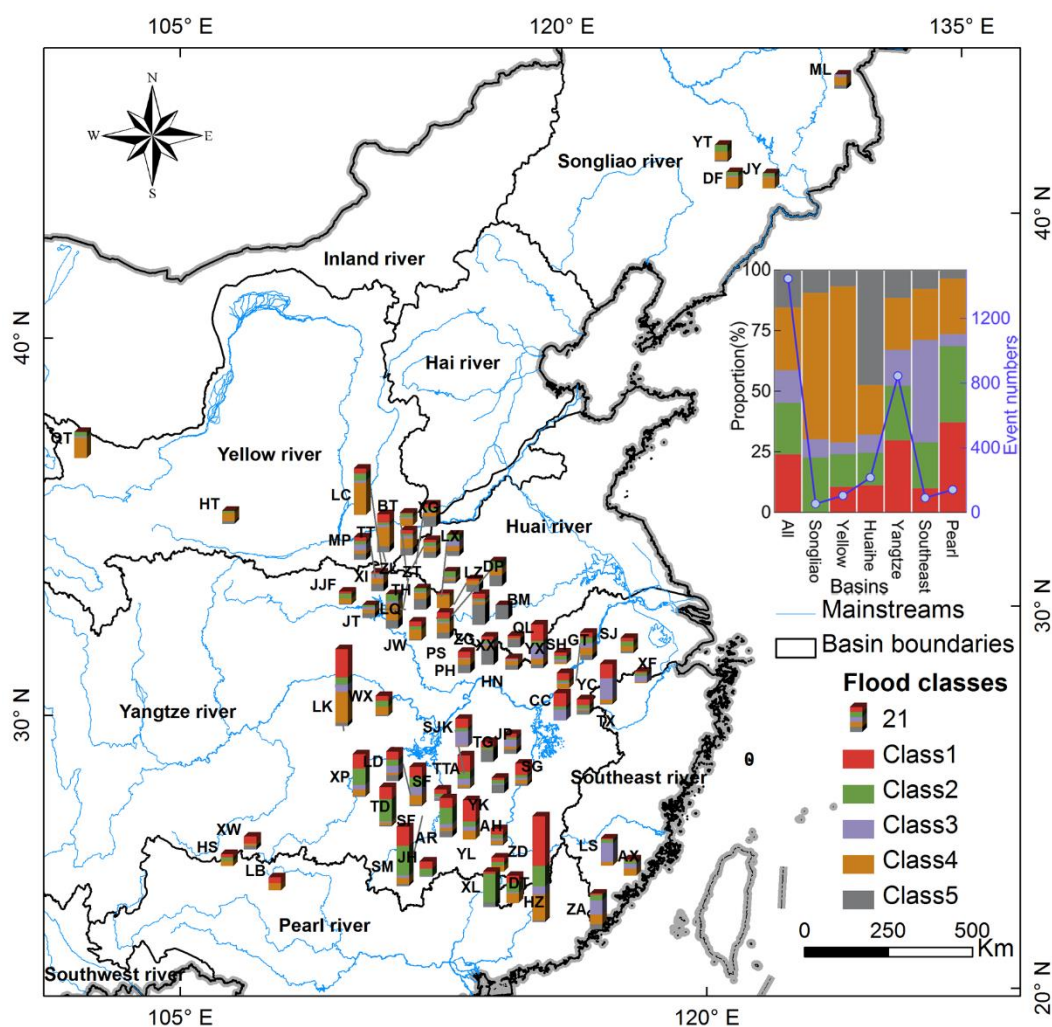


Figure 5. Spatial variabilities of individual flood event classes in major river basins

285

According to the interannual distributions of individual classes (Figure 6), all the classes are evenly distributed, whose annual mean percentages are $23.6 \pm 6.4\%$, $19.9 \pm 6.7\%$, $14.5 \pm 9.1\%$, $25.4 \pm 6.8\%$, and $16.6 \pm 9.1\%$, respectively. However, the interannual distributions of individual classes at the basin scale are quite distinct. In the Songliao River Basin, the dominant class is Class 4 with the annual mean percentage of $26.1 \pm 38.3\%$ though flood events are missed in several years due to the dry period. In the



290 Yellow River Basin, the Class 4 is also dominant across the whole period with the annual mean percentage of $58.1 \pm 33.9\%$, particularly in 1994-1996, 1999 and 2007. In the Huaihe River Basin, the Class 5 gradually prevail with the annual mean percentage of $41.5 \pm 23.7\%$, particularly after 2007, and the Classes 1 and 2 gradually decrease. In the Yangtze River Basin, the Classes 1 and 2 are dominant in the whole period, which account for $52.4 \pm 9.5\%$ of annual mean flood events, and their interannual distributions do not change considerably. In the Southeast River Basin, the Class 3 gradually prevail after 2000 with the annual mean percentage of $46.2 \pm 32.5\%$. In the Pearl River Basin, the Class 1 is dominant with the annual mean percentage of $36.0 \pm 24.0\%$, but gradually shifts to Class 2 which accounts for $30.0 \pm 25.2\%$ of annual mean flood events, particularly after 2008.

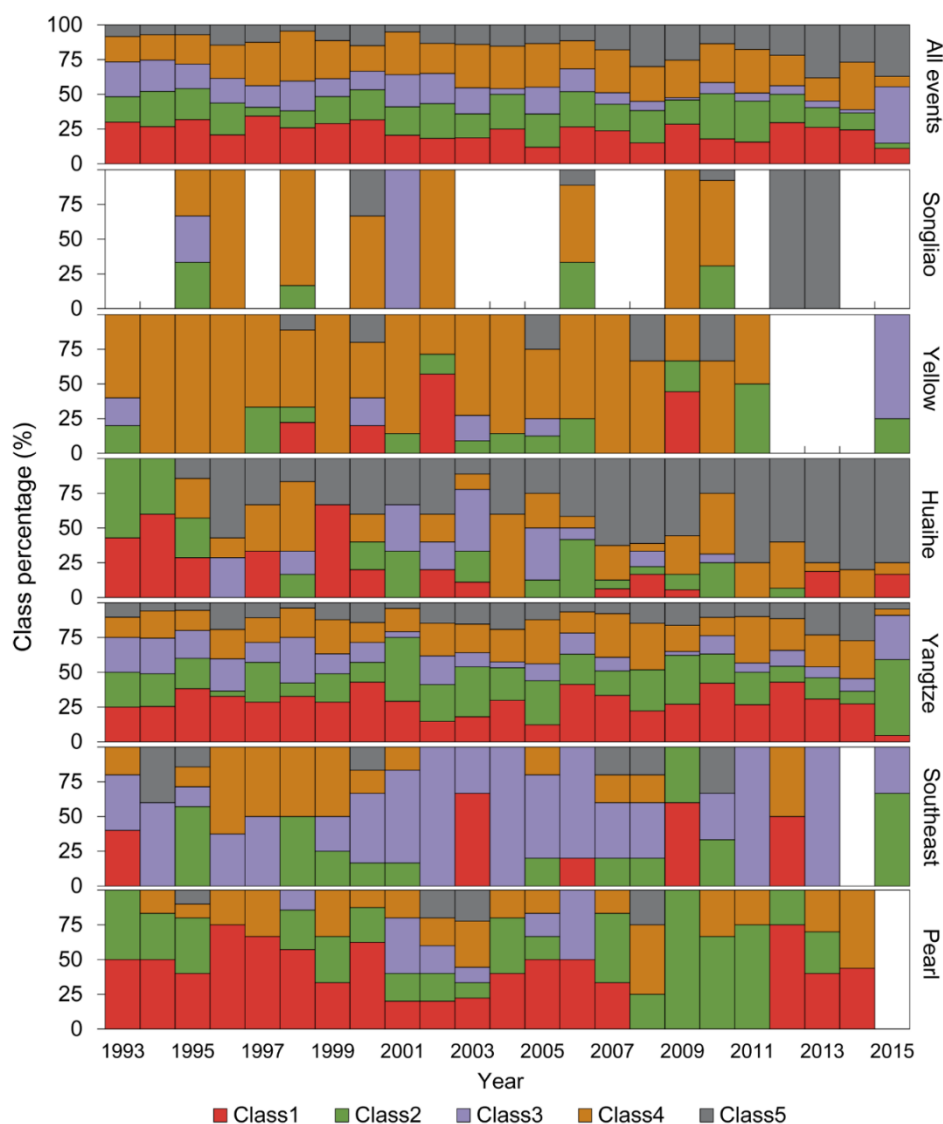


Figure 6. Interannual variabilities of individual flood event classes and their percentages in major river basins



300

4.4 Control mechanisms of meteorological and physio-geographical factors

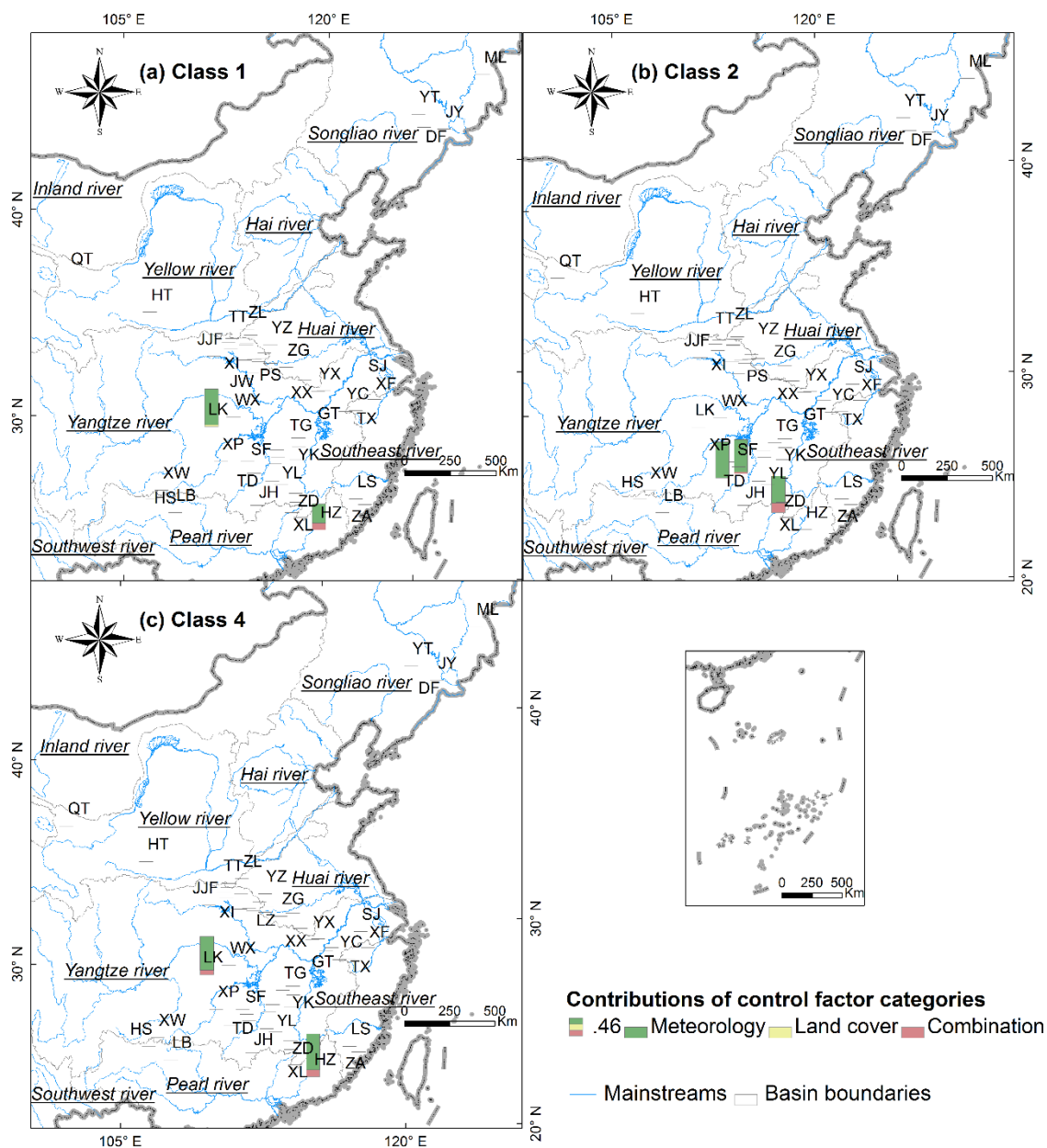
4.4.1 Control factors and their contributions for the distributed analysis

According to the Monte Carlo permutation test between flood behavior matrix and control factor matrix (i.e., meteorological and land cover categories) in the individual catchments (Figure 7), the significant control factors for the temporal variabilities of flood events in all the classes are mainly in the meteorological category, particularly the precipitation factors (e.g., volume, intensity) and aridity index during the events. In the Class 1, the total and mean precipitations, and aridity index during the event ($r_{pcp_dur}=0.65-0.99$, $n=14$; $r_{pcp_av}=0.70-0.97$, $n=7$; $r_{SPEI_dur}=0.52-0.97$, $n=7$) are the major control factors, particularly in the catchments of Yangtze River Basin. For the contributions of control factors, they are statistically significant only in the Liangshuikou (LK) catchment of the Yangtze River Basin and Hezikou (HZ) catchment of the Pearl River Basin (Figure 8). In the LK catchment, 96.3% of temporal differences are explained, in which the meteorological and land cover categories explain 92.5% and 3.8%, respectively. In the HZ catchment, 66.7% of temporal differences are explained, in which the meteorological category and the combined impact explain 49.4% and 17.3%, respectively.

In the Class 2, the significant control factors are mainly in the catchments of Pearl River Basin, particularly the total and mean precipitations, and aridity index during the event ($r_{pcp_dur}=0.61-0.99$, $n=9$; $r_{pcp_av}=0.58-0.99$, $n=6$; $r_{SPEI_dur}=0.50-0.98$, $n=5$). The contributions are statistically significant only in the Shimenkan (SM) and Tangdukou (TD) catchments of the Yangtze River Basin and Xiaogulu (XL) catchment of the Pearl River Basin. In the SM catchment, 90.7% of temporal differences are explained, in which the meteorological category and combined impact explain 87.1% and 3.8%, respectively. In the TD catchment, 95.9% of temporal differences are explained by the meteorological category. In the XL catchment, 96.8% of temporal differences are explained, in which the meteorological category and combined impact explain 71.9% and 24.9%, respectively.

In the Class 4, the significant control factors are mainly in the catchments of Yellow, Songliao and Pearl River Basins, particularly the total precipitation during the event, and the aridity index in the corresponding year ($r_{pcp_dur}=0.53-1.00$, $n=12$; $r_{SPEI_year}=0.45-0.93$, $n=6$). The contributions of meteorological and land cover categories are statistically significant only in the LK and HZ catchments. In the LK catchment, 87.0% of temporal differences are explained, in which the meteorological category and combined impact explain 72.8% and 10.2%, respectively. In the HZ catchment, 98.1% of temporal differences are explained, in which the meteorological category and the combined impact explains 82.1% and 16.0%, respectively.

In the Classes 3 and 5, the contributions of meteorological and land cover categories are not statistically significant in all the catchments because of the smaller numbers of flood events. However, several important control factors are also detected,

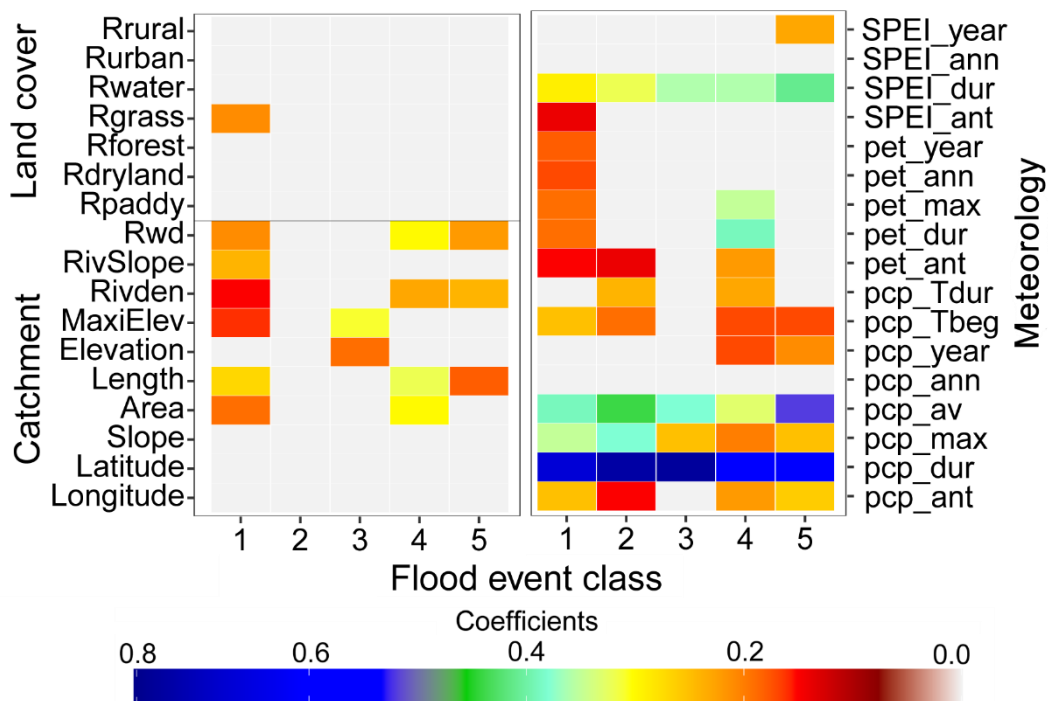


340 **Figure 8. Effect contributions of control factor categories on the temporal variabilities of flood event Classes 1, 2 and 4 (a,b,c) at catchment scale. Effect contributions in Classes 3 and 5 are not statistically significant.**



4.4.2 Control factors and their contributions for the lumped analysis

The Monte Carlo permutation tests across the entire study area suggest that the meteorological category is the most important (Figure 9), particularly the precipitation volume, intensity and the aridity index during the events with the correlation coefficients of 0.33-0.74, 0.20-0.38 and 0.29-0.41, respectively. The significant factor number in the catchment attribute category is less, which are mainly the mean catchment length, river density and ratio of river width to depth with the correlation coefficients of 0.18-0.32, 0.15-0.24 and 0.21-0.30, respectively. In the land cover category, only the grassland area ratio is significant in Class 1 with the correlation coefficient of 0.21.



350

Figure 9. Significant control factors and their correlation coefficients for the variabilities of individual flood event classes (i.e., Classes 1-5). The gray color means the control factor without statistical significance.

In the Class 1, the significant control factors are the meteorological factors in the antecedent seven days ($r_{pcp_ant}=0.25$, $r_{pet_ant}=0.15$ and $r_{SPEI_ant}=0.14$), during the events ($r_{pcp_dur}=0.67$, $r_{pcp_av}=0.39$, $r_{pcp_max}=0.35$, $r_{pcp_Tbeg}=0.25$, $r_{pet_dur}=0.19$, $r_{pet_max}=0.19$ and $r_{SPEI_dur}=0.29$), and at the annual scale ($r_{pet_ann}=0.17$ and $r_{pet_year}=0.18$) in the meteorological category, the catchment area ($r=0.19$), mean length ($r=0.27$), catchment maximum elevation ($r=0.16$), river density ($r=0.15$) and slope ($r=0.24$) and ratio of river width to depth ($r=0.21$) in the catchment attribute category, and the grassland area ratio ($r=0.21$) in the land cover category. There are 72.7% of total flood event differences explained by all the control factor categories, in which 43.9% of differences are explained by the meteorological category, followed by the combined impact (22.7%), land cover category (1.5%) and catchment attribute category (4.2%), respectively (Figure 10a).

360

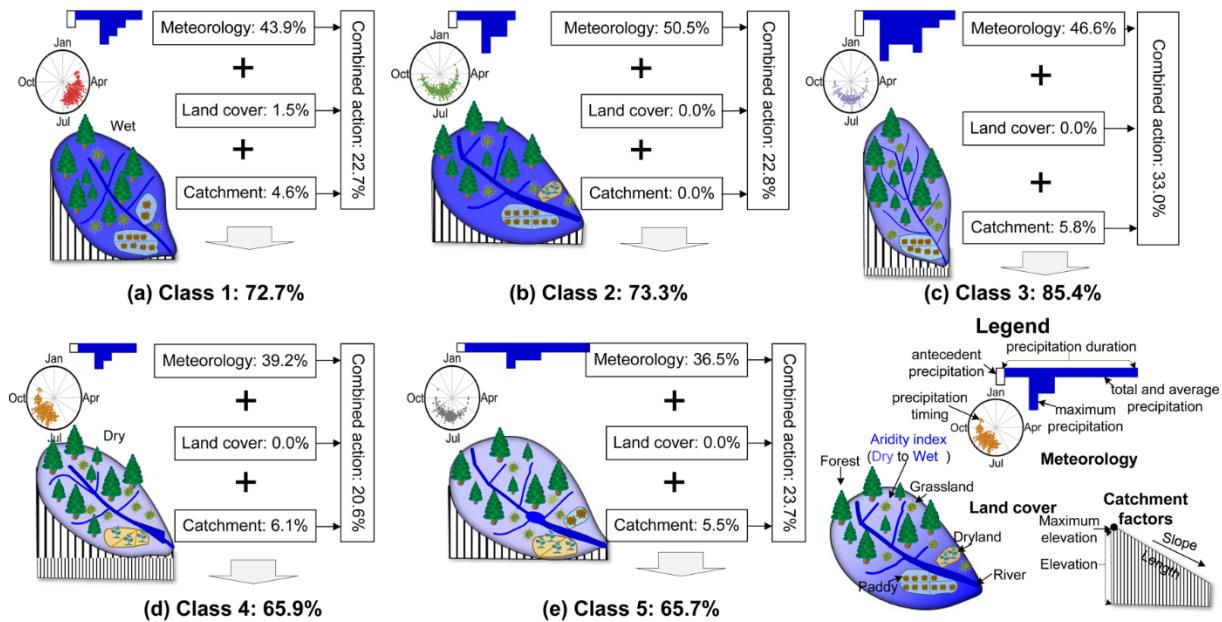


In the Class 2, the significant control factors are only in the meteorological category, including precipitation and potential evapotranspiration in the antecedent seven days ($r_{pcp_ant}=0.15$ and $r_{pet_ant}=0.14$), precipitation and aridity index during the flood
365 events ($r_{pcp_dur}=0.73$, $r_{pcp_av}=0.44$, $r_{pcp_max}=0.38$, $r_{pcp_Tbeg}=0.19$, $r_{pcp_Tdur}=0.24$ and $r_{SPEI_dur}=0.32$). There are 73.3% of total flood event differences explained by all the control factor categories, in which 50.5% of differences are explained by the meteorological category, followed by the combined impact (22.8%) (Figure 10b). The impacts of catchment attribute and land cover category are not significant.

370 In the Class 3, the significant control factors are the precipitation and aridity index during the flood events ($r_{pcp_dur}=0.74$, $r_{pcp_av}=0.38$, $r_{pcp_max}=0.25$, and $r_{SPEI_dur}=0.36$) in the meteorological category, and the catchment center elevation ($r=0.19$) and maximum elevation ($r=0.31$) in the catchment attribute category. There are 85.4% of total flood event differences explained by all the control factor categories, in which 46.6% of differences are explained by the meteorological category, followed by the combined impact (33.0%) and catchment attribute category (5.8%), respectively (Figure 10c). The impact of land cover
375 category is not significant.

In the Class 4, the significant control factors are the precipitation and potential evapotranspiration in the antecedent seven days ($r_{pcp_ant}=0.22$ and $r_{pet_ant}=0.22$), precipitation, potential evapotranspiration and aridity index during the events ($r_{pcp_dur}=0.56$, $r_{pcp_av}=0.33$, $r_{pcp_max}=0.20$, $r_{pcp_Tbeg}=0.17$, $r_{pcp_Tdur}=0.23$, $r_{pet_dur}=0.39$, $r_{pet_max}=0.35$, and $r_{SPEI_dur}=0.36$) and at the annual scale
380 ($r_{pcp_year}=0.17$) for the meteorological attribute category, and the catchment area ($r=0.30$), mean length ($r=0.32$), river density ($r=0.23$) and ratio of river width to depth ($r=0.30$) in the catchment attribute category. There are 65.9% of total flood event differences explained by all the control factor categories, in which 39.2% of differences are explained by the meteorological category, followed by the combined impact (20.6%) and catchment attribute category (6.1%), respectively (Figure 10d). The impact of land cover category is also not significant.

385 In the Class 5, the significant control factors are the precipitation in the antecedent seven days ($r_{pcp_ant}=0.26$), precipitation, potential evapotranspiration and aridity index during the events ($r_{pcp_dur}=0.59$, $r_{pcp_av}=0.52$, $r_{pcp_max}=0.25$, $r_{pcp_Tbeg}=0.17$ and $r_{SPEI_dur}=0.41$) and at the annual scale ($r_{pcp_year}=0.21$ and $r_{SPEI_year}=0.23$) for the meteorological attribute category, and the catchment mean length ($r=0.18$), river density ($r=0.24$) and ratio of river width to depth ($r=0.22$) in the catchment attribute
390 category. There are 65.7% of total flood event differences explained by all the control factor categories, in which 36.5% of differences are explained by the meteorological category, followed by the combined impact (23.7%) and catchment attribute category (5.5%), respectively (Figure 10e). The impact of land cover category is also not significant.



395 **Figure 10.** Effect contributions of control factor categories on the spatial and temporal variabilities of flood event classes 1-5 (a-e)

4.4.3 Control mechanisms in the individual flood event classes

In both the individual catchments and the entire region, the dominant control factors of all the flood event classes are the total and mean precipitation volumes, the maximum precipitation intensity, the aridity index and the precipitation timing during the events, the precipitation in the antecedent days in the meteorological category. Therefore, the flood events in Class 1 are mainly caused by the rainfall with low volume and intensity before the wet season in the wet, steep and low-latitude catchments (Figure 11). The events in Class 2 are mainly caused by the short rainfall with high mean intensity in the wet low-latitude catchments. The events in Class 3 are mainly caused by the long rainfall with high volume and intensity in the small catchments of high altitude and low latitude. The events in Class 4 are mainly caused by the short rainfall with low volume and intensity in the latter wet season in the dry, steep and small catchments of high altitude and latitude. The events in Class 5 are mainly caused by the long rainfall with high volume and low mean intensity in the dry, gentle and large mid-latitude catchments.

400

405

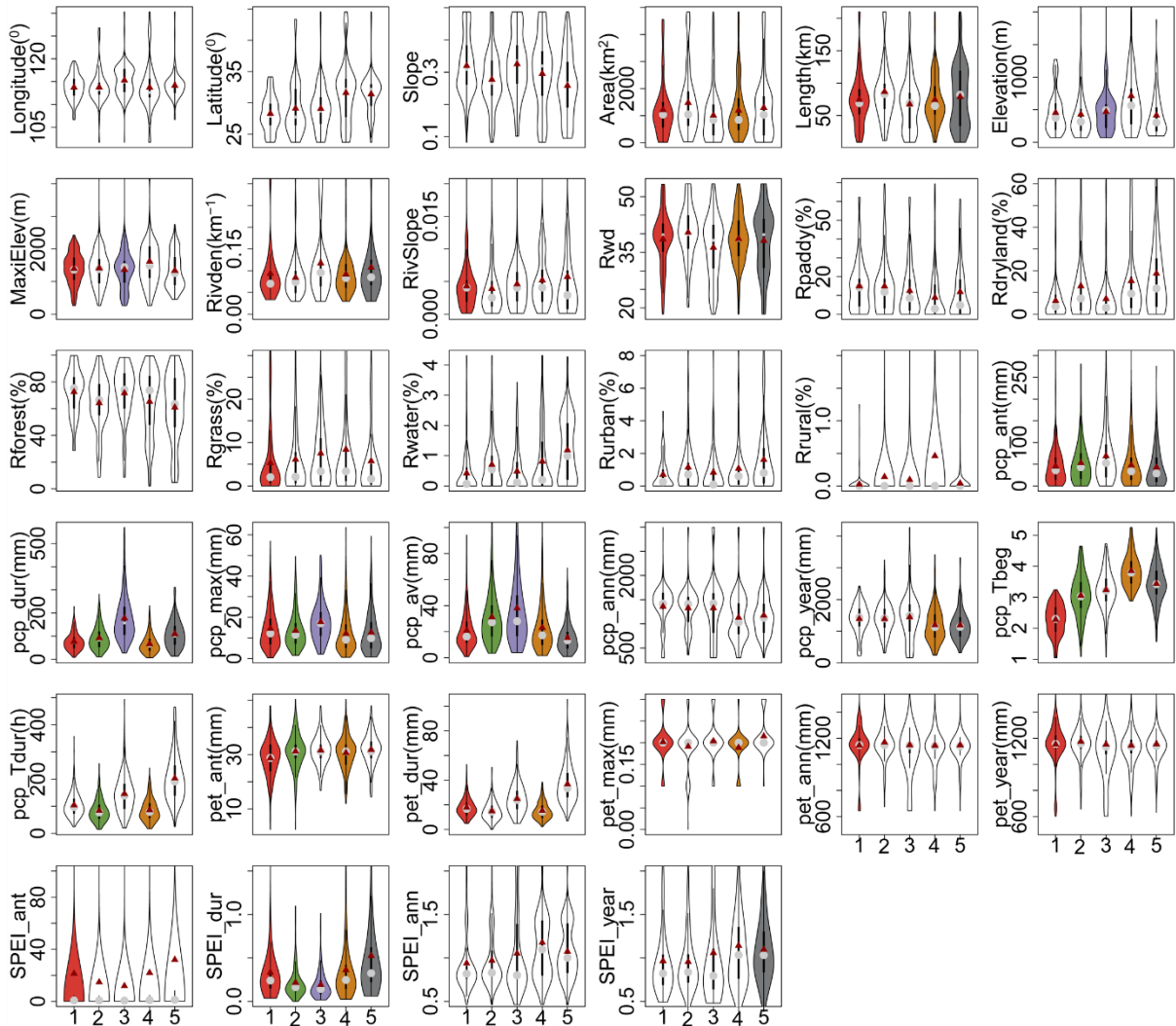


Figure 11. Variations of control factors among Classes 1-5. The solid darkred dot and gray dot define the mean and 50th percentile values, respectively. Each black box means the 25th and 75th percentile values, and the vertical line defines the minimum and maximum values without outliers. The violin shape means the frequency distribution of control factor, and the unfilled shape means the control factor without statistically significant.

410

5. Discussion

Flood classification has strong advantages in systematically identifying manageable classes from a large number of historical flood events based on the similarity of flood behavior characteristics (Arthington *et al.*, 2006; Kuentz *et al.*, 2017; Poff *et al.*, 2007; Sikorska *et al.*, 2015; Sivakumar *et al.*, 2015). Flood events in the same class are widely accepted to have similar hydrological behaviors caused by similar meteorological or underlying surface conditions (Sikorska *et al.*, 2015). Therefore,

415



it is more efficient to investigate flood event changes and their cause mechanisms in a comprehensive manner than individual event analyses (Zhang *et al.*, 2012). It is expected to provide more useful flood behavior characteristics for flood disaster management purposes (e.g., early warning and quick design of flood control plans) and provide deep insights to investigate riverine ecological and environmental response mechanisms.

In our study, the flood event classes are identified based on the entire flood behavior characteristics, which cover not only the flood magnitude metrics, e.g., large, moderate and small floods but also the event shape metrics, e.g., fast or slow floods. Therefore, our study captures more detailed behavior dynamics of flood events than the predefined classes reported by several existing studies, such as flash floods, short-rain floods, rain-on-snow floods or snowmelt floods (Brunner *et al.*, 2018; Merz and Blöschl, 2003; Sikorska *et al.*, 2015). Classes 1 and 2 are mainly in southern China and are controlled by the temperate climate without a dry season. Storms with high intensities and short durations are likely to cause flood events with great magnitudes and variabilities (Class 1) or fast flood events with a high single peak and short durations (Class 2). The flood behavior characteristics in these two classes are similar to flash floods and short-rain floods in Austria and Europe (Merz and Blöschl 2003; Sikorska *et al.*, 2015), spike floods in Europe (Kuentz *et al.*, 2017), and fast events in Switzerland (Brunner *et al.*, 2018) and China (Zhai *et al.*, 2021). Class 3 is mainly in the Southeast River Basin controlled by the subtropical southeast monsoon climate. Severe subtropical storms with high intensities and durations are likely to cause high slow flood events with multiple peaks (Class 3) (Zhang *et al.*, 2020). The flood behavior characteristics are similar to the high unit peak flood in the west coast of the USA (Saharia *et al.*, 2017) and the slow events in Switzerland (Brunner *et al.*, 2018) and China (Zhai *et al.*, 2021). Class 4 is mainly in northern China and is controlled by the cold climate with dry winters. The dominant storms with low intensities and short durations in the latter wet season are likely to cause small fast flood events (Class 4). A similar flood event class is also reported, e.g., the low flashiness floods in Europe (Kuentz *et al.*, 2017). Class 5 is mainly in the south–north climate zone of China, which has the dual climate characteristics of both south and north monsoons. Storms characterized by a long period of continuous rainy meteorological with high frequency and low intensities (e.g., Meiyu rainfalls) are likely to cause moderate slow flood events with long durations (Sampe and Xie, 2010). The flood behavior characteristics are similar to those of long-rain floods (Merz and Blöschl, 2003) or bimodal floods (Hall and Blöschl, 2018) in Europe. Therefore, the classification is helpful to deeply investigate the control mechanisms of flood events, which is easy to transfer to predict flood events with similar control factors (Sikorska *et al.*, 2015).

The meteorological, land cover and catchment attribute categories are mainly reported to affect the flood generation and routing processes, and could be widely-accepted as the critical control factors of spatial and temporal differences of flood event classes (Ali *et al.*, 2012; Brunner *et al.*, 2018; Merz and Blöschl, 2003; Zhang *et al.*, 2022). Our results also find that the meteorological category is dominant, which explain 49.4%-95.9% and 36.5%-50.5% of the flood event differences in individual classes at catchment scale and in the entire region, respectively. Similar results were also reported in Kuentz *et al.* (2017). The main significant meteorological factors are the precipitation volume, intensity and the aridity index during the events. The main



455 explanation is that the precipitation and aridity index during the flood events directly affect the hydrograph through flood
generation, e.g., total volume and peak, variability, duration, rate of changes and peak number (Merz and Blöschl, 2003;
Aristeidis *et al.*, 2010). Additionally, these control factors in the antecedent days directly affect the antecedent soil moisture,
which determine the initial losses of precipitation and the runoff generation timing during the flood events (Hall and Blöschl,
460 2018; Xu *et al.*, 2023). Secondly, the catchment attributes (e.g., geographical location and topography) mainly affect the
hydrograph patterns through flood routing (Berger and Entekhabi, 2001; Ali *et al.*, 2012;), and the identified factors in our
study are the catchment area and length, river density and ratio of river width to depth. For example, a catchment with longer
routing length, larger routing area, river density and ratio of river width to depth usually has larger flood regulation and storage
capacity, and thus generates the slow flood events, while a catchment with shorter routing length, smaller routing area, river
465 density and ratio of river width to depth usually has weaker flood regulation and storage capacity, and thus generates the fast
flood events (Zhang *et al.*, 2020). However, the comprehensive contributions of catchment attributes are not considerable, i.e.,
only 0.0%-6.1% in the entire region because the catchment attributes do not always well match the flood event behaviors
(Kuentz *et al.*, 2017; Ali *et al.*, 2012). Furthermore, the location, annual precipitation, potential evapotranspiration and aridity
index mainly affect the overall catchment hydrological conditions (Berger *et al.*, 2001; Kennard *et al.*, 2010). Finally, the land
470 covers mainly determine the precipitation intercept and retention processes, which directly affect the flood variability and rate
of changes (Kuentz *et al.*, 2017; Merz *et al.*, 2020). For example, catchments with greater vegetation covers (e.g., forest,
grassland) usually generate the slow flood events, while catchments with weaker vegetation covers (e.g., rural and urban lands)
usually generate the fast flood events (Kuentz *et al.*, 2017; Zhai *et al.*, 2021). However, all the catchments selected in our
study are mainly in the river source regions with good vegetation coverages with mean area percentages of 67.0% for forest
475 and 6.6% for grassland. The spatial and temporal differences of land covers are not remarkable so that it only explains 3.8%
and 1.5% of the flood event differences in Class 1 at the Liangshuikou catchment of Yangtze River Basin and in the entire
region, respectively.

480 However, several limitations should be noted in our study. Firstly, total flood event number is the main restricted factor for
the classification performance, the flood event class representativeness and their control mechanisms at catchment scale (Merz
and Blöschl, 2003; Olden *et al.*, 2012; Sikorska *et al.*, 2015; Tarasova *et al.*, 2020). It could be overcome effectively by
adopting the minimum flood event numbers of individual classes (i.e., 10% of total events in our study) for the classification
(Zhang *et al.*, 2020). However, not all the control mechanisms of flood event classes were well explained because of the
insufficient flood events, which were mainly in the Songliao and Yellow River Basins, or most catchments expect the
485 Shimenkan, Liangshuikou and Tangdukou catchments of the Yangtze River Basin, Xiaogulu and Hezikou catchments of the
Pearl River Basin. Secondly, the class boundaries of most flood behavior metrics were not clear using the inductive
classification approaches (Parajka *et al.*, 2005; Sikorska *et al.*, 2015), e.g., the flood magnitude, rates of positive and negative
changes in our study. Although the predefined sharp thresholds of all the flood behavior metrics are beneficial to clearly
separate the flood events using the classification tree methods (e.g., decision tree, crisp tree), the predefinition is still



485 challenging (Sikorska *et al.*, 2015; Brunner *et al.*, 2017; Tarasova *et al.*, 2020). Finally, the control mechanism deduction was
mainly based on the statistical detection of control factors and their contributions. The combined impacts of different control
factor categories were still difficult to be clearly explained using the adopted statistical analysis method (i.e., the constrained
rank analysis in our study).

6. Conclusions

490 In our study, the main flood event classes characterized by multiple flood behavior metrics are identified in 68 headstream
catchments using the hierarchical and partitional clustering methods. The control mechanisms of different flood event classes
are investigated using the constrained rank analysis and Monte Carlo permutation test. Results are summarized as follows: the
partitional clustering method (i.e., *k*-medoids) performs better than the hierarchical method, and the optimal five flood event
classes are identified which are the moderately fast flood event class (Class 1), the highly fast flood event class (Class 2), the
495 highly slow and multipeak flood event class (Class 3), the slightly fast flood event class (Class 4) and the moderately slow
flood event class (Class 5). Most of the flood event differences among individual classes are explained by the meteorological,
land cover and catchment attribute factors. The flood event differences in Class 3 (85.4%) are well explained, followed by
Classes 2 (73.3%), 1 (72.7%), 4 (65.9%) and 5 (65.7%). The meteorological category is the most significant among all the
control factors, particularly the precipitation factors (e.g., volume, intensity) and aridity index during the flood events.

500

This study preliminarily investigates the flood event classes in space and time in China, which is beneficial to explore the
comprehensive formation mechanisms of flood events and the critical control factors, and provides the scientific foundation
for flood event prediction and control. In future, more unimpacted flood events could be collected to strengthen the
representativeness of flood event classes, and to further support the control mechanism analysis of flood classes at individual
505 catchments. The combined impacts of control factor categories could also be further decomposed into the impacts of individual
factors using the hydrological model with strong physical mechanism.

Acknowledgements

This study was supported by the National Natural Science Foundation of China (Nos. 41671024 and 42171047) and the
National Key Research and Development Program of China (No. 2021 YFC3201102).

510



Author contribution

Yongyong Zhang: Conceptualization, Methodology, Formal Analysis, Writing-Original draft preparation, Writing-Reviewing and Editing, Funding acquisition; **Yongqiang Zhang:** Conceptualization, Writing-Reviewing and Editing; **Xiaoyan Zhai:** Data curation, Formal Analysis, Writing-Reviewing and Editing, Funding acquisition; **Jun Xia:** Conceptualization, Writing-
515 Reviewing and Editing; **QiuHong Tang:** Conceptualization, Writing-Reviewing and Editing; **Wei Wang:** Data Processing, Formal Analysis; **Jian Wu:** Formal Analysis; **Xiaoyu Niu:** Formal Analysis; **Bing Han:** Formal Analysis

Code/Data availability

The geographic information system data sources are obtained from the Data Center of Resources and Environmental Science, Chinese Academy of Sciences (<http://www.resdc.cn/>). The historical flood events and synchronous precipitation are collected
520 from the Hydrological Yearbooks of the Songliao, Yellow, Huaihe, Yangtze, Southeast and Pearl River Basins which are published by the Ministry of Water Resources of the People's Republic of China (http://xxfb.mwr.cn/sq_djdh.html).

Competing interests

The authors declare no conflicts of interest relevant to this study.

References

- 525 Ali, G., Tetzlaff, D., Soulsby, C., McDonnell, J. J., and Capell, R.: A comparison of similarity indices for catchment classification using a cross-regional dataset, *Adv. Water Resour.*, 40, 11–22, <https://doi.org/10.1016/j.advwatres.2012.01.008>, 2012.
- Antoine, L. and Sylvain J.: Using amap and ctc Packages for Huge Clustering. *R News*, 6(5):58-60, 2006.
- Aristeidis, G. K., Tsanis, I. K., and Daliakopoulos, I. N.: Seasonality of floods and their hydrometeorologic characteristics in
530 the island of Crete, *J. Hydrol.*, 394(1–2), 90-100, <https://doi.org/10.1016/j.jhydrol.2010.04.025>, 2010
- Arthington, A. H., Bunn, S. E., Poff, N. L., and Naiman, R. J.: The challenge of providing environmental flow rules to sustain river ecosystems, *Ecological Applications*, 16, 1311–1318, [https://doi.org/10.1890/1051-0761\(2006\)016\[1311:TCOPEF\]2.0.CO;2](https://doi.org/10.1890/1051-0761(2006)016[1311:TCOPEF]2.0.CO;2), 2006
- Berger, K. P., and Entekhabi, D.: Basin hydrologic response relations to distributed physiographic descriptors and climate, *J.*
535 *Hydrol.*, 247(3-4), 169-182. [https://doi.org/10.1016/S0022-1694\(01\)00383-3](https://doi.org/10.1016/S0022-1694(01)00383-3), 2001
- Brunner, M. I., Viviroli, D., Furrer, R., Seibert, J., and Favre, A. C.: Identification of flood reactivity regions via the functional clustering of hydrographs, *Water Resour. Res.*, 54, 1852-1867. <https://doi.org/10.1002/2017WR021650>, 2018



- Brunner, M. I., Viviroli, D., Sikorska, A. E., Vannier, O., Favre, A.C., and Seibert, J.: Flood type specific construction of synthetic design hydrographs, *Water Resour. Res.*, 53,1390–1406, <https://doi.org/10.1002/2016WR019535>, 2017.
- 540 Charrad, M., Ghazzali, N., Boiteau, V., and Niknafs, A.: NbClust: An R package for determining the relevant number of clusters in a data set, *J. Stat. Softw.*, 61(6), 1-36, <http://hdl.handle.net/10.18637/jss.v061.i06>,2014
- Hall, J., and Blöschl, G.: Spatial patterns and characteristics of flood seasonality in Europe, *Hydrol. Earth Syst. Sc.*, 22, 3883–3901, <https://doi.org/10.5194/hess-22-3883-2018>, 2018.
- Hargreaves, G. H., and Samani, Z. A.: Estimating potential evapotranspiration, *J. Irrig. Drain. Div.*, 108(3), 225-230, 545 [https://doi.org/10.1016/0022-1694\(82\)90165-2](https://doi.org/10.1016/0022-1694(82)90165-2),1982.
- Hartigan, J. A., and Wong, M. A.: Algorithm AS 136: A K-means clustering algorithm, *Appl. Stat.*, 28, 100–108, <https://doi.org/10.2307/2346830>, 1979.
- Hirabayashi, Y., Mahendran, R., Koirala, S., Konoshima, L., Yamazaki, D., Watanabe, S., Kim, H., and Kanae, S.: Global flood risk under climate change, *Nat. Clim. Change*, 3, 816–821. <https://doi.org/10.1038/NCLIMATE1911>, 2013.
- 550 Jongman, B. Winsemius, H. C., Aerts, J. C. J. H., Coughlan de Perez, E., van Aalst, M. K., Kron, W., and Ward, P. J.: Declining vulnerability to river floods and the global benefits of adaptation, *P. Natl. Acad. Sci. USA*, 112, E2271–E2280. <https://doi.org/10.1073/pnas.1414439112>, 2015.
- Kaufman, L. and Rousseeuw, P.J.: *Finding Groups in Data: An Introduction to Cluster Analysis*. Wiley, New York,1990.
- Kennard, M. J., Pusey, B. J., Olden, J. D., Mackay, S. J., Stein, J. L., and Marsh, N.: Classification of natural flow regimes in 555 Australia to support environmental flow management, *Freshwater Biol.*, 55, 171–193. <https://doi.org/10.1111/j.1365-2427.2009.02307.x>, 2010
- Kuentz, A., Arheimer, B., Hundsdoerfer, Y., and Wagener, T.: Understanding hydrologic variability across Europe through catchment classification, *Hydrol. Earth Syst. Sc.*, 21, 2863–2879. <https://doi.org/10.5194/hess-21-2863-2017>, 2017.
- Legendre, P., and Anderson, M. J.: Distance-based redundancy analysis: testing multispecies responses in multifactorial 560 ecological experiments, *Ecol. Monogr.*, 69(1), 1-24, [https://doi.org/10.1890/0012-9615\(1999\)069\[0001:DBRATM\]2.0.CO;2](https://doi.org/10.1890/0012-9615(1999)069[0001:DBRATM]2.0.CO;2), 1999.
- Liu, J.Y., Feng, S.Y., Gu, X.H., Zhang, Y.Q., Beck, H.E., Zhang, J.W., and Yan, S.: Global changes in floods and their drivers, *J. Hydrol.*, 614, 128553. <https://doi.org/10.1016/j.jhydrol.2022.128553>, 2020
- Mardia, K. V., Kent, J. T., and Bibby, J. M.: *Multivariate Analysis*, London, Academic Press, 1979.
- 565 Merz, R., and Blöschl, G.: A process typology of regional floods, *Water Resour. Res.*, 39(12), 1340. <https://doi.org/10.1029/2002WR001952>, 2003.
- Merz, R., Tarasova, L., and Basso, S.: The Flood Cooking Book: ingredients and regional flavors of floods across Germany, *Environ. Res. Lett.*, 15(11), 114024, <https://doi.org/10.1088/1748-9326/abb9dd>, 2020.
- Ministry of Water Resources of the People’s Republic of China: Bulletin of flood and drought disasters in China from 2009 to 570 2018. China Water & Power Press. Retrieved from <http://www.mwr.gov.cn/sj/tjgb/zgshzhgb/>, 2020a.



- Ministry of Water Resources of the People's Republic of China: Code for hydrologic data processing (SL/T 247—2020), 2020b.
- Olden, J. D., Kennard, M. J., and Pusey, B. J.: A framework for hydrologic classification with a review of methodologies and applications in ecohydrology, *Ecohydrology*, 5, 503–518. <https://doi.org/10.1002/eco.251>, 2012.
- 575 Parajka, J., Merz, R., and Blöschl, G.: A comparison of regionalization methods for catchment model parameters, *Hydrol. Earth Syst. Sc.*, 9, 157–171. <https://doi.org/10.5194/hess-9-157-2005>, 2005.
- Peel, M. C., Finlayson, B. L., and McMahon, T. A.: Updated world map of the Köppen-Geiger climate classification, *Hydrol. Earth Syst. Sc.*, 11, 1633–1644. <https://doi.org/10.5194/hess-11-1633-2007>, 2007.
- Poff, N.L., Allan, J.D., Bain, M.B., Karr, J.R., Prestegard, K.L., Richter, B.D., Sparks, R.E., and Stromberg, J.C.: The natural
580 flow regime: a paradigm for river conservation and restoration, *Bioscience*, 47, 769–784, 10.1080/09647778409514905, 1997.
- Poff, N. L., and Zimmerman, J. K. H.: Ecological responses to altered flow regimes: a literature review to inform environmental flows science and management, *Freshwater Biol.*, 55, 194–205, <https://doi.org/10.1080/09647778409514905>, 2010.
- Poff, N. L., Olden, J. D., Merritt, D., and Pepin, D.: Homogenization of regional river dynamics by dams and global
585 biodiversity implications, *P. Natl. Acad. Sci. USA*, 104, 5732–5737. <https://doi.org/10.1073/pnas.0609812104>, 2007.
- R Development Core Team: R: A language and environment for statistical computing. Vienna, Austria: R Foundation for Statistical Computing. Retrieved from <http://www.R-project.org>, 2010.
- Richter, B.D., Baumgartner, J.V., Powell, J., Braun, D.P.: A method for assessing hydrological alteration within ecosystems, *Conserv. Biol.*, 10(4): 1163–1174, <https://doi.org/10.1046/j.1523-1739.1996.10041163.x>, 1996.
- 590 Rustomji, P., Bennett, N., and Chiew, F.: Flood variability east of Australia's great dividing range, *J. Hydrol.*, 374(3-4), 196–208. <https://doi.org/10.1016/j.jhydrol.2009.06.017>, 2009.
- Saharia, M., Kirstetter, P. E., Vergara, H., Gourley, J. J., and Hong, Y.: Characterization of floods in the United States, *J. Hydrol.*, 548, 524–535. <https://doi.org/10.1016/j.jhydrol.2017.03.010>, 2017.
- Sampe, T., and Xie, P.: Large-scale dynamics of the Meiyu baiu rainband: Environmental forcing by the westerly jet. *Journal*
595 *of Climate*, 23, 113–133, <https://doi.org/10.1175/2009JCLI3128.1>, 2010.
- Shi, P., Zhang, Y., Li, Z., Li, P., and Xu, G.: Influence of land use and land cover patterns on seasonal water quality at multi-spatial scales, *Catena*, 151, 182–190, <https://doi.org/10.1016/j.catena.2016.12.017>, 2017.
- Sikorska, A. E., Viviroli, D. and Seibert, J.: Flood-type classification in mountainous catchments using crisp and fuzzy decision trees, *Water Resour. Res.*, 51, 7959–7976. <https://doi.org/10.1002/2015WR017326>, 2015.
- 600 Sivakumar, B., Singh, V., Berndtsson, R., and Khan, S.: Catchment classification framework in hydrology: challenges and directions, *J. Hydrol. Eng.*, 20, A4014002. [https://doi.org/10.1061/\(ASCE\)HE.1943-5584.0000837](https://doi.org/10.1061/(ASCE)HE.1943-5584.0000837), 2015
- Tarasova, L., Basso, S., Wendi, D., Viglione, A., Kumar, R., and Merz, R.: A process-based framework to characterize and classify runoff events: The event typology of Germany, *Water Resour. Res.*, 56, e2019WR026951, 2020.



- 605 ter Braak, C. J. F.: Canonical Correspondence Analysis: a new eigenvector technique for multivariate direct gradient analysis, *Ecology*, 67, 1167-1179, <https://doi.org/10.2307/1938672>, 1986.
- Xu, Z., Zhang, Y., Blöschl, G., and Piao, S.: Mega forest fires intensify flood magnitudes in southeast Australia, *Geophys. Res. Lett.*, 50, e2023GL103812. <https://doi.org/10.1029/2023GL103812>, 2023.
- Zhai, X. Y., Guo, L., and Zhang, Y. Y.: Flash flood type identification and simulation based on flash flood behavior indices in China, *Sci. China Earth Sci.*, 64(7), 1140–1154. <https://doi.org/10.1007/s11430-020-9727-1>, 2021.
- 610 Zhang, S.L., Zhou, L.M., Zhang, L., Yang, Y.T., Wei, Z.W., Zhou, S., Yang, D.W., Yang, X. F., Wu, X.C., Zhang, Y.Q., and Dai, Y.J.: Reconciling disagreement on global river flood changes in a warming climate, *Nat. Clim. Change*, 12, 1160–1167, <https://doi.org/10.1038/s41558-022-01539-7>, 2022.
- Zhang, Y. Y., Arthington, A. H., Bunn, S. E., Mackay, S., Xia, J., and Kennard, M.: Classification of flow regimes for environmental flow assessment in regulated rivers: the Huai River Basin, China, *River Res. Appl.*, 28, 989–1005, <https://doi.org/10.1002/rra.1483>, 2012.
- 615 Zhang, Y., Zhou, Y., Shao, Q., Liu, H., Lei, Q., Zhai, X., and Wang, X.: Diffuse nutrient losses and the impact factors determining their regional differences in four catchments from North to South China, *J. Hydrol.*, 543, 577-594, <https://doi.org/10.1016/j.jhydrol.2016.10.031>, 2016.
- Zhang, Y. Y., Chen, Q. T., and Xia, J.: Investigation on flood event variations at space and time scales in the Huai River Basin of China using flood behavior classification, *J. Geogr. Sci.*, 30(12), 2053-2075. <https://doi.org/10.1007/s11442-020-1827-3>, 2020.
- 620